IEEE Access
Multidisciplinary | Rapid Review | Open Access Journal

Received January 28, 2021, accepted February 17, 2021, date of publication February 22, 2021, date of current version March 3, 2021.

Digital Object Identifier 10.1109/ACCESS.2021.3060749

Fuzzy Multilevel Image Thresholding Based on Improved Coyote Optimization Algorithm

LINGUO LI[1,2], LIJUAN SUN[1], YU XUE[3], (Member, IEEE), SHUJING LI[2], XUWEN HUANG[4], AND ROMANY FOUAD MANSOUR[5]

[1]School of Computer, Nanjing University of Posts and Telecommunications, Nanjing 210003, China
[2]College of Information Engineering, Fuyang Normal University, Fuyang 236041, China
[3]School of Computer and Software, Nanjing University of Information Science and Technology, Nanjing 210044, China
[4]College of Computer and Information Engineering, Fuyang Normal University, Fuyang 236041, China
[5]Department of Mathematics, Faculty of Science, New Valley University, El-Kharga 72511, Egypt

Corresponding author: Shujing Li (lsjing1981@163.com)

This work was supported in part by the National Youth Natural Science Foundation of China under Grant 61802208; in part by the National Natural Science Foundation of China under Grant 61873131 and Grant 61876089; in part by the Natural Science Foundation of Anhui under Grant 1908085MF207 and Grant KJ2020A1215; in part by the Excellent Youth Talent Support Foundation of Anhui under Grant gxyqZD2019097; in part by the Postdoctoral Foundation of Jiangsu under Grant 2018K009B; in part by the Higher Education Quality Project of Anhui under Grant 2019sjjd81, Grant 2018mooc059, and Grant 2018kfk009; in part by the Industry-University Cooperation Collaborative Education Foundation under Grant 201901258002; and in part by the Fuyang Normal University Doctoral Startup Foundation under Grant 2017KYQD0008.

ABSTRACT Due to the computational complexity of multilevel image thresholding, Swarm Intelligence Optimization Algorithm (SIOA) has been widely applied to improve the calculation efficiency. Therefore, more and more attention has been paid to exploring the application of the latest SIOA in multilevel segmentation. This article takes Otsu and fuzzy entropy as the objective functions, using Coyote Optimization Algorithm (COA) for multilevel thresholds optimization selection, through fuzzy median aggregation of local neighborhood information and then forms the Fuzzy Coyote Optimization Algorithm (FCOA), so that the thresholding image segmentation can be achieved in the end. To prevent the COA algorithm from falling into the local optimum, this article follows the differential evolution strategy adopted by the standard COA, using the number of iterations to construct the differential scaling factor to form the Improved Coyote Optimization Algorithm (ICOA). The experimental results show that fuzzy Kapur entropy and fuzzy median value aggregation-based ICOA(FICOA) achieves better image segmentation quality. Compared with Grey Wolf Optimizer (GWO), Fuzzy Modified Quick Artificial Bee Colony and Aggregation Algorithm (FMQABCA) and Fuzzy Modified Discrete Grey Wolf Optimizer and Aggregation Algorithm (FMDGWOA), FCOA and FICOA have certain advantages in visual effects of image segmentation and PSNR, FSIM evaluation indices. Particularly compared with GWO (also a wolf evolutionary algorithm), FICOA shows significant advantages.

INDEX TERMS Coyote optimization algorithm, information entropy, image segmentation, multilevel thresholding.

I. INTRODUCTION

Thresholding image segmentation divides the original image into two or more adjacent regions that do not intersect by setting different threshold numbers [1]. It is a main method and important branch of image segmentation, widely used in image and video compression [2]–[4], image denoising [5], [6], document processing [7], and target recognition [8], [9], etc. According to the number of thresholds, thresholding image segmentation can be divided into two categories: bilevel thresholding and multilevel thresholding (MT) [10]. Bilevel thresholding divides the image into two regions: foreground and background, while the multilevel thresholding divides the image into several homogeneous or adjacent pixel groups (i.e., regions) with common features. As the threshold number increases, the computational complexity of these methods also increases dramatically. Therefore, a large number of swarm intelligence optimization algorithms (SIOA) are applied to improve the computational efficiency [11].

The associate editor coordinating the review of this manuscript and approving it for publication was Zhaoqing Pan.

According to the difference of thresholds applied in the range of image, thresholding techniques can be divided into global thresholding and local thresholding [12]. The global thresholding method selects a threshold in the whole image histogram, while the local thresholding method selects the thresholds individually in a relatively small set of regions to complete the multilevel thresholding. By comparison, the global thresholding is simpler and easier to implement, but the segmentation results are directly controlled by the global threshold. While the local thresholding method is more precise, its computational complexity is higher. Whether global thresholding or local thresholding is applied, the computing methods can be divided into two categories: parametric methods and non-parametric methods. Parametric methods need to estimate a large number of statistical parameters, and the segmentation results are heavily dependent on the initial conditions. Therefore, non-parametric methods have been applied increasingly [13]. Non-parametric methods select the optimal threshold by calculating some specific criteria, such as Otsu or Kapur, Tsallis, etc. As a result, with the increase of threshold number, multilevel thresholding selection will become a NP-hard problem [14]. In such cases, SIOA provides an effective solution.

With specific SIOA, the optimal threshold value in thresholding segmentation can be obtained efficiently according to image histogram and specific objective function [10]. In our previous work, we use artificial bee colony algorithm [13] and gray wolf algorithm [14] to explore the effect of MT image segmentation. This article will analyze and discuss the application of coyote algorithm in MT segmentation. According to our designed framework same as [13] and [14], the MT segmentation based on the intelligence optimization algorithm is mainly divided into three steps: (1) select the objective function. (2) based on the objective function, select or improve the certain SIOA, so as to obtain the optimal threshold and complete the initial segmentation of the original image. (3) optimize the initial segmentation results, which can be performed according to the threshold numbers, and then apply local neighborhood information aggregation to complete the regional segmentation.

The purpose of thresholding image segmentation is to separate regions of interest from background or other complex scenes by setting different thresholds. To this end, non-parametric methods based on image histogram are widely used to design objective functions [11]. In recent years, a large number of alternative schemes have appeared. Aziz *et al.* [10] analyzed the application of Otsu objective function in MT segmentation on eight Berkeley standard data sets with the help of WOA (Whale Optimization Algorithm) and MFO (Moth Flame Optimization). Büranur Küükuurlu *et al.* [15] discussed the application of SOS (Symmetric Organizations Search Algorithm) with Kapur entropy and Otsu as objective functions. Experimental results show that Kapur function-based SOS, Otsu function-based SOS and PSO (particle swarm optimization) can obtain more stable results, while FA (Firefly Algorithm) and GA (Genetic Algorithm) are relatively poor. In the Friedman test, the optimization effect of Kapur entropy-based SOS proved the best, and GWO (grey wolf optimizer) based on these two objective functions had more advantages in processing speed. Elazi *et al.* [16] verified the application of GA and other four kinds of meta-heuristic algorithms in MT image segmentation. Unfortunately, the authors only verified the efficiency of Otsu as the objective function, but failed to provide the experimental data and results about Kapur's entropy. Xing [17] used Kapur's entropy as the objective function to verify that the EPO (Emperor Penguin Optimization) algorithm had higher segmentation accuracy and less running time on plant canopy and satellite images. He and Huang [18] applied Kapur's entropy, Tsallis entropy and Otsu respectively to explore the effectiveness of KH (Krill Herd) algorithm. Experiment results indicate that Kapur's entropy performs better in precision and robustness. Wu *et al.* [19] used Kapur and Otsu as objective functions, and obtained the optimal threshold through the teaching–learning-based optimization algorithm. Statistical analysis shows that Kapur's entropy is better in mean values and standard deviation, while Otsu is better in time efficiency. Naidu *et al.* [20] compared with DE (Differential Evolution), PSO and BA ((Bat Algorithm), they found that FA (Fire Algorithm) with Shannon entropy and fuzzy entropy as objective functions, performs best in SSI (Structural Similarity Index), PSNR (Peak Signal to Noise Ratio), ME (Misclassification Error) and processing time.

Based on the above analysis and summary of the non-parametric objective functions used in MT segmentation in recent years, we find it is still necessary to select an appropriate optimization algorithm to solve the problem of computational efficiency. Yang and Wu [21] used NRQPSO (Non Revising Quantum Behaved Particle Swarm Optimization) algorithm to test the application of MT method on gray images with Kapur objective function. The experimental results show that the algorithm can effectively avoid the repeated calculation of the objective function and effectively reduce calculation cost of the algorithm. Bhandari *et al.* [22] analyzed the effects of PSO, WDO (Wind Driven Optimization), DE and CS (Cuckoo Search) in satellite image segmentation. Statistical analysis shows that the four optimization algorithms achieve similar segmentation results, CS algorithm obtains slightly higher objective function values of Kapur and Otsu, while DE algorithm is better than three other algorithms in time efficiency. Tarkhaneh and Shen [23] improved the global search performance of DE algorithm using Lévy and Cauchy distribution, and verified the segmentation effect of MRI brain images in combination with Otsu method. Compared with other improved DE algorithms, this algorithm achieves better thresholding value under the condition that the calculation time can be controlled effectively. Zhang *et al.* [24] improved the ABC (Artificial Bee Colony) algorithm by using Krill Herd algorithm, which adopts Kapur entropy as the objective function on the basis of image preprocessing. Compared with other improved ABC

algorithms, this algorithm is better in PSNR and FSIM statistical parameters. In [13], we improved the ABC algorithm, using PTS (Pseudo Trapezoid Shaped Function) to assign fuzzy membership, and then using median, mean and iterative means to aggregate information to form FMQABCA algorithm. Compared with EMO (electro magnet optimization), ABC and DE, FMQABCA can obtain the optimal threshold quickly, efficiently and accurately, especially in time efficiency. Using Kapur entropy and Ostu as objective functions, the efficiency of GWO algorithm in MT image segmentation is tested by Khairuzzaman and Chaudhury [25]. Compared with PSO and BFO (Bacterial Forecasting Optimization) algorithm, this method is more stable and can provide a higher quality segmentation solution. In addition, the authors find that such method is faster than BFO in processing speed, but slower than PSO. In [14], we improved the grey wolf optimizer using fuzzy Kapur entropy as the objective function. In the algorithm, discrete GWO is defined firstly, and after the optimal threshold is obtained, the neighborhood information aggregation is achieved by fuzzy initialization, similar to that in [13]. The experimental results showed that FMDGWOA is superior to EMO, standard GWO algorithm and FDE (Fuzzy Differential Evolution Algorithm).

So far, the objective function and related swarm intelligence optimization algorithms used in image segmentation in recent years have been analyzed respectively [11]. In terms of objective function, Kapur and Otsu are still the two most widely used. While SIOA is in bloom, various heuristic intelligent optimization algorithms are emerging, and a considerable number of algorithms have been successfully applied in MT segmentation. These commonly used algorithms include DE, ABC, GWO, PSO and many improved algorithms corresponding to them, which also further proves that the use of SIOA to obtain the optimal threshold is still of significant research necessity and remains a hot topic. The results of MT image segmentation in recent years reveal that although there has been great improvement in segmentation quality, segmentation accuracy, and time cost, a considerable number of segmentation algorithms are prone to produce fuzzy boundaries, and even more so, isolated points [11], [13], [14]. Furthermore, heuristic algorithms still have capacity for improvement in balancing exploration and exploitation [26]. Therefore, in [13], [14], we try to use fuzzy objective function and fuzzy aggregation method in MT segmentation, and obtain better segmentation accuracy and segmentation effect. This article will continue to explore the effect of COA in thresholding image segmentation based on the existing framework in [13], [14].

The COA [27] is inspired by canis latrans species that mainly lives in North America. The social organization of the coyotes and their adaptability to the environment are mainly considered in the algorithm design. Compared with GWO algorithm (also inspired by canis latrans species), it provides a different algorithm structural setup. Even though the alpha is still regarded as the leader of the wolf pack (optimal threshold), it focuses less on the social hierarchy of these coyotes, dominance rules and the way they hunt, but more on the social structure and experience exchanges among them, so as to achieve better exploration and exploitation. Since Pierezan *et al.* proposed the algorithm in 2018, Souza *et al.* [28] applied COA to image feature selection, Sultan *et al.* [29] used COA to select parameters in fuel cell model, and Arfaoui *et al.* [30] used COA to improve the performance of solar photovoltaic water pump system. Unfortunately, so far there has been no application of COA in MT image segmentation. In this article we will for the first time explore the effect of the improved COA which are used the Fuzzy Kapur entropy and Otsu in multilevel thresholding, and through fuzzy median aggregation [13], [14] forms the Fuzzy Coyote Optimization Algorithm (FCOA), then the FCOA is further improved to form FICOA.

The remainder of this article is organized as follows: in the second section, Otsu method is formulated, fuzzy Kapur entropy and the final objective function are briefly introduced. In the third section, the detailed process of the standard COA and the improved COA proposed in this article are presented. In the fourth section, the segmentation results and detailed data comparison of the proposed method are analyzed and summarized comprehensively. Finally, the fifth section contains the conclusions and the prospects of the future research.

II. ANALYSIS AND FORMULATION OF OBJECTIVE FUNCTION

Non-parametric methods generally use the probability distribution of the image gray level i to design the objective function. In this article, we use fuzzy Kapur entropy and Otsu as the objective functions. As the fuzzy Kapur entropy has been described in detail in [13], [14], so we will only present the Otsu method. In multilevel thresholding image segmentation, k thresholds can be used to segment the image into $k+1$ regions. The statistical probability of each gray level of the image is assumed to be h_i, the probability distribution function can be expressed as:

$$p_i = h(i) \Big/ \sum_{i=0}^{n} h(i), \quad i = 0, 1, \cdots, n \tag{1}$$

where n is the maximum gray level (less than 255) of image. According to the probability distribution function in (1), the Otsu objective function in MT is defined as:

$$f(T) = \sum_{i=0}^{k} \sigma_i \tag{2}$$

where $T = [t_1, t_2, \cdots, t_k]$ is the threshold vector composed of K thresholds, σ_i represents the inter-class variance in different regions, which is formulated as:

$$\begin{cases} \sigma_0 = \omega_0(\mu_0 - \mu_T)^2 \\ \sigma_1 = \omega_1(\mu_1 - \mu_T)^2 \\ \sigma_i = \omega_i(\mu_i - \mu_T)^2 \\ \vdots \\ \sigma_{k-1} = \omega_{k-1}(\mu_{k-1} - \mu_T)^2 \end{cases} \tag{3}$$

where ω_i is the probability distribution of the *i-th* region, as shown in (4), μ_i is the average probability of the *i-th* region, as shown in (5), and μ_T is the average probability density of the whole image.

$$\begin{cases} \omega_0 = \sum_{i=0}^{t_1-1} p_i, \quad \omega_1 = \sum_{i=t_1}^{t_2-1} p_i \\ \omega_j = \sum_{i=t_j}^{t_{j+1}-1} p_i \\ \vdots \\ \omega_{k-1} = \sum_{i=t_k}^{n} p_i \end{cases} \tag{4}$$

$$\begin{cases} \mu_0 = \sum_{i=0}^{t_1-1} \frac{ip_i}{\omega_0}, \quad \mu_1 = \sum_{i=t_1}^{t_2-1} \frac{ip_i}{\omega_1} \\ \mu_j = \sum_{i=t_j}^{t_{j+1}-1} \frac{ip_i}{\omega_j} \\ \vdots \\ \mu_{k-1} = \sum_{i=t_k}^{n} \frac{ip_i}{\omega_{k-1}} \end{cases} \tag{5}$$

Taking Otsu and fuzzy Kapur as the objective functions, the COA and ICOA are used to optimize the threshold vector, then achieves image segmentation through the obtained optimal thresholds, and finally refines the segmentation results through neighborhood pixel aggregation same as references 13 and 14.

III. APPLICATION OF THE IMPROVED COA IN MULTILEVLEL IMAGE THRESHOLDING

A. THE PARAMETER SETTING AND DISCUSSION OF COA IN MULTILEVEL IMAGE THRESHOLDING

The COA builds an algorithm model based on the coyote population structure and environmental adaptability. In the algorithm, the coyote population is divided into N_p packs, with each pack containing N_i coyotes, thus making a total of $N_i^* N_p$ different coyotes. Usually the swarm intelligence optimization algorithm only sets one group. So the main purpose of the multigroup structure in COA is to simulate the population structure of coyotes to facilitate population mutation and cross-fusion. In the nature, coyotes generally form a family structure with the head coyote as the leader, and each family competes and continuously merges with each other to adapt to the environment and complete the hunting. In order to simplify the algorithm model, solitary coyotes and short-lived small populations are not considered during initialization, furthermore, each coyote represents a threshold vector in MT segmentation, which is constantly updated and eliminated according to the objective function during the population iteration process.

In the process of model construction, COA constructs its population according to intrinsic and extrinsic factors. The intrinsic factors mainly include the packs, population status and sex, while external factors mainly consider temperature, snow thickness, snow hardness, and prey number. In multilevel thresholding segmentation, a threshold vector is randomly initialized by the population according to the value range of the image gray level (between 0-255), so the *i-th* threshold vector (population) of the *p-th* pack is an integer vector at a certain time t, it is formulated as follows:

$$S_i^{p,t} = (x_1, x_2, \cdots x_d) \tag{6}$$

where d is the dimension of the optimized problem, that is, the number of thresholds, x_i is the *i-th* threshold.

The first step in the COA is to initialize the population by randomly initializing each x_i in (6), as can be shown in (7):

$$S_{i,j}^{p,t} = lb_j + random_j \cdot (ub_j - lb_j), \quad j = 1, 2, \cdots, d \tag{7}$$

where lb_j and ub_j represent the lower and upper bounds of the gray level of the image, which are 0 and 255 respectively, $random_j$ is a random value inside the range [0, 1] that conforms to the standard probability distribution. Since all gray levels of the image are integers, all thresholds that are randomly generated need to be rounded during initialization.

Next, we need to evaluate the newly generated population during each initialization or iteration process to determine whether the population is updated or eliminated. In specific cases, it is generally reduced to a fitness function, such as equation (8), where *fit* is the fitness evaluation function. In this algorithm, fuzzy Kapur entropy and Otsu are used as the fitness evaluation functions, such that:

$$f_{i,j}^{p,t} = fit(S_{i,j}^{p,t}) \tag{8}$$

The randomly initialized population is randomly assigned to different packs. According to the COA, each coyote can leave or be evicted from its pack, becomes a solitary one or joins a pack. In this work, the standard COA strategy will be followed, and the probability of coyote leaving or being evicted can be written as:

$$P_e = 0.005 \cdot N_i^2 \tag{9}$$

To prevent the probability value from exceeding 1, the number of coyotes per pack is limited to 14. This mechanism ensures that the population can be combined freely, which not only reflects the diversity of the population, but also indirectly improves the global optimal performance of the algorithm. In the continuous iterative process of population optimization, each iteration will select an optimal threshold (the optimal population) according to the objective function, which is formulated as:

$$best^{p,t} = \left\{ S_i^{p,t} \left| \arg_{i=1,2,\cdots d} \max fit(S_i^{p,t}) \right. \right\} \tag{10}$$

As one kind of higher-order social mammals, coyotes form a well-organized pack by sharing social environment, knowledge and experience, and contribute to the packs' survival and development. In order to accurately reflect the packs'

social environment and knowledge and experience exchange pattern, the COA collects the social behavior of all coyotes and computes it as the cultural tendency of the pack:

$$cult_j^{p,t} = \begin{cases} O^{p,t}_{\frac{N_i+1}{2},j}, & N_i \text{ is odd} \\ \dfrac{O^{p,t}_{\frac{N_i}{2},j} + O^{p,t}_{\frac{N_i}{2}+1,j}}{2}, & otherwise \end{cases} \tag{11}$$

where $O^{p,t}_{i,j}$ represents the social conditions (social environment, knowledge and experience, etc.) of the *j-th* component of the *p-th* pack.

In order to maintain the diversity of the population, new threshold vectors must be generated continuously in the iterative process to prevent the algorithm from falling into the local optimum. COA simulates the breeding behavior of coyote pack by continuously generating pups. Parents of young coyote are randomly selected from the population and some environmental factors are applied, as shown in (12).

$$\begin{cases} pup_j^{p,t} = S^{p,t}_{r_1,j}, & rand_j < P_s or j = j_1 \\ S^{p,t}_{r_2,j}, & rand_j \geq P_s + P_a or j = j_2 \\ R_j, & otherwise \end{cases} \tag{12}$$

where r_1 and r_2 are the sequence numbers of two randomly initialized packs, j_1 and j_2 are the sequence numbers of two randomly initialized intra population dimensions, i.e., the parents of pups, P_s and P_a are the scatter probability and the association probability, respectively, as shown in (13) and (14). R_j is a random value in the gray level range of an image, and $rand_j$ is a random number inside the range of 0 to 1.

$$P_s = 1/D \tag{13}$$

$$P_a = (1 - P_s)/2 \tag{14}$$

Under natural conditions, the pups have 10% chances of dying, and the adult coyotes will also die with the increase of age. In order to keep the population number stable, COA sets ω and ϕ to eliminate the population with low objective function value in the iterative process. In this work the population elimination mechanism of standard COA is applied. Meanwhile, in order to reflect the cross-mutation in the pack, the standard COA sets up two influence factors and promotes the generation of new populations, as shown in (15) and (16), where cr_1 and cr_2 are two random numbers, that is, by using two randomly selected threshold vectors $S^{p,t}_{cr_1}$ and $S^{p,t}_{cr_2}$ to differentiate them from the current optimal threshold vector $best^{p,t}$ and the social conditions $cult^{p,t}$ of the pack:

$$\delta_1 = best^{p,t} - S^{p,t}_{cr1} \tag{15}$$

$$\delta_2 = cult^{p,t} - S^{p,t}_{cr1} \tag{16}$$

With the two influence factors δ_1 and δ_2, the new threshold vector (new population) is initialized by two random numbers between 0 and 1, as shown in (17). After the new threshold vector is initialized, its fitness value is computed according to equation 8 and then updated according to equation 18

$$NS_i^{p,t} = S_i^{p,t} + r_1 \cdot \delta_1 + r_2 \cdot \delta_2 \tag{17}$$

$$S_i^{p,t+1} = \begin{cases} NS_i^{p,t}, & fit(NS_i^{p,t}) > fit(S_i^{p,t}) \\ S_i^{p,t}, & otherwise \end{cases} \tag{18}$$

B. THE APPLICATION OF IMPROVED COA(ICOA) IN MULTILEVEL IMAGE THRESHOLDING

From the equations (10) and (17) in standard COA, it can be seen that the updating of the optimal threshold is completed by the current optimal individual $best^{p,t}$ and the current thresholds $S^{p,t}$ through differential mutation, that is, the other individuals in the population are guided by $best^{p,t}$ towards the optimal threshold. After numerical iterations, almost all the other individuals move close to the current optimal individual in the later stage, creating a clustering phenomenon. Under normal circumstances, the algorithm will gradually move towards the optimal thresholds, but if $best^{p,t}$ falls into the local optimum, then premature convergence will appear, that is, the local optimum. In order to make the algorithm stay clear of the local optimum, it is necessary to find a way out. The general method to solve this problem is to introduce mutation operation to enhance the ability of the algorithm to avoid local optimum. Therefore, differential operation is used in this work to improve COA to form an improved COA, i.e. ICOA

Inspired by the standard COA's differential mutation strategy, we adopt a special differential dynamical mutation perturbation strategy to differentiate between r_1 and r_2 in (17), and design an adaptive differential scaling factor F to enhance its ability of avoiding local optimum. The specific expression is as follows:

$$F_{r1} = ((1 - t/t_{\max})(1 - r_1 \cdot t/t_{\max}))^3 \tag{19}$$

$$F_{r2} = ((1 - t/t_{\max})(1 - r_2 \cdot t/t_{\max}))^3 \tag{20}$$

where t is the current iteration number, $t_{\max}$ is the largest iteration number, r_1 and r_2 are the random numbers inside the range [0,1]. Thus, the equation for the newly generated population in (17) is changed into the following:

$$NS_i^{p,t} = S_i^{p,t} + F_{r1} \cdot \delta_1 + F_{r2} \cdot \delta_2 \tag{21}$$

With such improvement, the population$NS^{p,t}$ not only realizes the pairwise differential mutation among current threshold $S^{p,t}$, optimal threshold $best^{p,t}$ and cultural tendency $cult^{p,t}$, but also changes their corresponding scaling factors F_{r1} and F_{r2} from an ordinary random number to differential scaling factors which are jointly produced by random numbers and iteration times.

IV. COMPARISON AND ANALYSIS OF EXPERIMENTAL RESULTS

A. THE PARAMETER SETTING AND RELATED DISCUSSION FOR ANALYSIS OF EXPERIMENTAL RESULTS

According to the parameter setting of the standard COA [27], combined with the characteristics of multilevel thresholding image segmentation, and based on a large number of experimental tests, the number of test thresholds in this study is

TABLE 1. Parameter setting.

Parameter	No. of Packs	Coyotes per Pack	No. of Thresholds	No. of iterations
Value	20	5	2,3,4,5	10000

set to 2,3,4 and 5, and the number iterations set to are 10000, as shown in Table 1:

In the standard COA, the authors have fully discussed the algorithm performance under different parameter conditions, and have provided relatively excellent parameter selections, such as the number of packs and the number of coyotes in each pack are set to 20 and 5 respectively. In this article, by combining the characteristics of thresholding image segmentation, we will further optimize the relevant parameter setting through experimental comparison. As in [13], [14], the number of thresholds is set to 2,3,4 and 5. The number of iterations is set to 10000, and the number of iterations in standard COA is set to 10000 * D (D is the dimension of the problem). Through experimental comparison, and taking into account the time efficiency and segmentation quality of the algorithm, we find that the objective function tends to stabilize with 10000 iterations. The specific parameter comparison is shown in Table 2.

TABLE 2. Image segmentation quality with different no. of iterations.

No. of iterations	1000	3000	5000	10000	20000
PSNR	20.4205	20.5556	20.5698	20.6468	20.5795
FSIM	0.6670	0.6875	0.6888	0.6916	0.6931

Table 2 shows the PSNR and FSIM image segmentation quality evaluation parameters when the threshold number of the Srub image in Figure 1 is 5 and the objective function is fuzzy Kapur entropy. An introduction to the PSNR parameters can be found in [13], and FSIM is also a measurement standard to measure the feature similarity between the original image and segmented image features. These two parameters are currently popular image segmentation quality evaluation parameters [11], [31], detailed definition of FSIM parameters can be found in [22]. From the comparison of the two parameters in Table 2, when the number of iterations increases from 1000 to 10000, both PSNR and FSIM also increase to varying degrees. However, after the number of iterations reaches 20000, PSNR begins to decrease, and FSIM increases but slightly. And in terms of time efficiency, when the number of iterations is 20000, the running time of the program is 13.940412 seconds, while 10000 iterations only take 7.278475 seconds. Therefore, considering the two factors of running time and segmentation quality, the iteration number is determined to be 10000.

The data sets used in our work are from Berkeley Segmentation Data Set BSD500 [13], [14], as shown in Figure 1. The

FIGURE 1. The original images for multilevel image thresholding.

experiments are run on HP ProDesk 400 G4 PC with the Intel Core i5 processor and Matlab2016a. Based on the thresholds obtained by ICOA, the image is grayscaled firstly and then segmented according to the thresholds, after that, we adopt the framework in [13], [14], using the PTS membership function to realize neighbor-hood fuzzy aggregation to improve the accuracy of image segmentation.

Figure 2 shows the segmentation results of Fighter under different aggregation methods. Table 3 lists the relevant PSNR values by different aggregation methods. It can be seen from the data comparison in Table 3 that median aggregation has achieved the best segmentation effect, so the subsequent experimental results and data are obtained by median aggregation.

TABLE 3. Comparation of different aggregation method by PSNR.

MT	2	3	4	5
Median	**17.0304**	**20.2354**	**21.3911**	**21.8223**
Average	17.0098	20.1165	21.0691	21.1892
Iterative Average	16.9711	20.0271	20.9738	21.3052

Our work not only presents the image segmentation results, but also analyzes the segmentation quality in a quantitative manner. As the framework used in this article is similar to that in [13], [14], our proposed method will be compared with FMQABCA [13] and FMDGWOA [14] using PSNR and

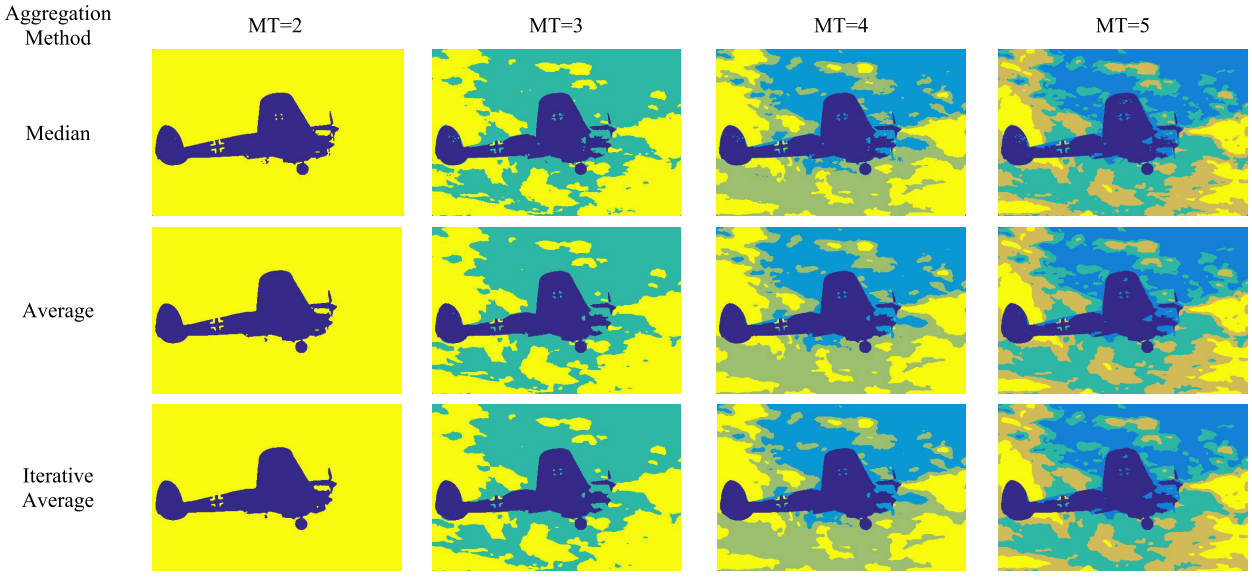

FIGURE 2. The segmentation results of FICOA by different aggregation methods.

FSIM evaluation indices. Meanwhile, GWO as an optimized design based on the wolf pack is also used in MT image segmentation in [25], therefore, this article will also be compared with it.

B. THE FUZZY MULTILEVEL IMAGE THRESHOLDING ANALYSES BASED ON FICOA AND OTSU OBJECTIVE FUNCTION

Otsu and Kapur entropy are still the most widely used objective functions in multilevel thresholding image segmentation in recent years [11]. Table 4 lists the relevant threshold values optimized by FICOA and the PSNR and FSIM values after fuzzy median aggregation of the six images is completed, as shown in Figure 1. with Otsu as the objective function, when the thresholds are set to 2, 3, 4 and 5, we observe that with the increase of the number of thresholds, the thresholds at all levels are more evenly distributed inside the range of 0 to 255 gray levels. From the PSNR and FSIM evaluation indices for image segmentation, it can be seen that with the increase of the threshold number, these two evaluation indices will also increase, thus the image segmentation quality can be improved when the number of thresholds increases. This section only lists the relevant parameter values, and the detailed comparative analysis with other methods will be presented in the following sections.

C. THE FUZZY MULTILEVEL IMAGE THRESHOLDING ANALYSES BASED ON FICOA AND FUZZY KAPUR OBJECTIVE FUNCTION

In [13], [14], we have comprehensively analyzed the advantages and disadvantages of Kapur entropy and fuzzy Kapur entropy. Obviously, fuzzy Kapur entropy has greater advantages. In this work, we also find that the image segmentation results based on fuzzy entropy are better in FICOA through

TABLE 4. The results of FICOA with Otsu objective function.

Image	MT	Thresholds	PSNR	FSIM
Fighter	2	97 157	**17.7418**	**0.7069**
	3	94 146 188	19.3901	0.7117
	4	93 140 172 204	20.1571	**0.7235**
	5	92 138 163 187 211	20.5990	0.7419
Goose	2	84 174	**18.9572**	0.5910
	3	75 131 196	22.5731	0.6171
	4	45 80 133 196	24.0963	0.6829
	5	44 71 109 151 202	25.1372	0.7298
Shrub	2	125 173	18.4331	**0.4695**
	3	112 151 174	19.7837	**0.5993**
	4	92 125 155 174	20.3121	**0.6425**
	5	93 117 140 159 174	20.4713	0.6698
Community	2	94 154	18.1574	0.5456
	3	64 116 163	19.9675	0.6199
	4	54 96 133 169	**20.7524**	**0.6688**
	5	50 89 124 156 181	21.2715	0.7083
Starfish	2	89 157	**17.4951**	0.5093
	3	80 135 188	19.3622	**0.5939**
	4	69 112 151 197	21.1208	0.6253
	5	54 89 127 164 206	22.5662	0.7156
Picnic	2	123 193	**18.4021**	**0.5848**
	3	108 154 210	**20.9162**	**0.6651**
	4	95 128 168 218	22.6975	0.7260
	5	89 117 149 183 224	23.8422	0.7683

experiments, Therefore, in the following comparative analysis with other MT image segmentation methods, this article will focus on the advantages of our algorithm using fuzzy Kapur entropy as show in Figure 3 and Figure 4.

Table 5 lists the experimental data based on FICOA and fuzzy Kapur entropy with different threshold numbers. From the comparison between Table 4 and Table 5, it can be seen that when the threshold number is 2, the Otsu method achieves relatively higher segmentation quality (PSNR and

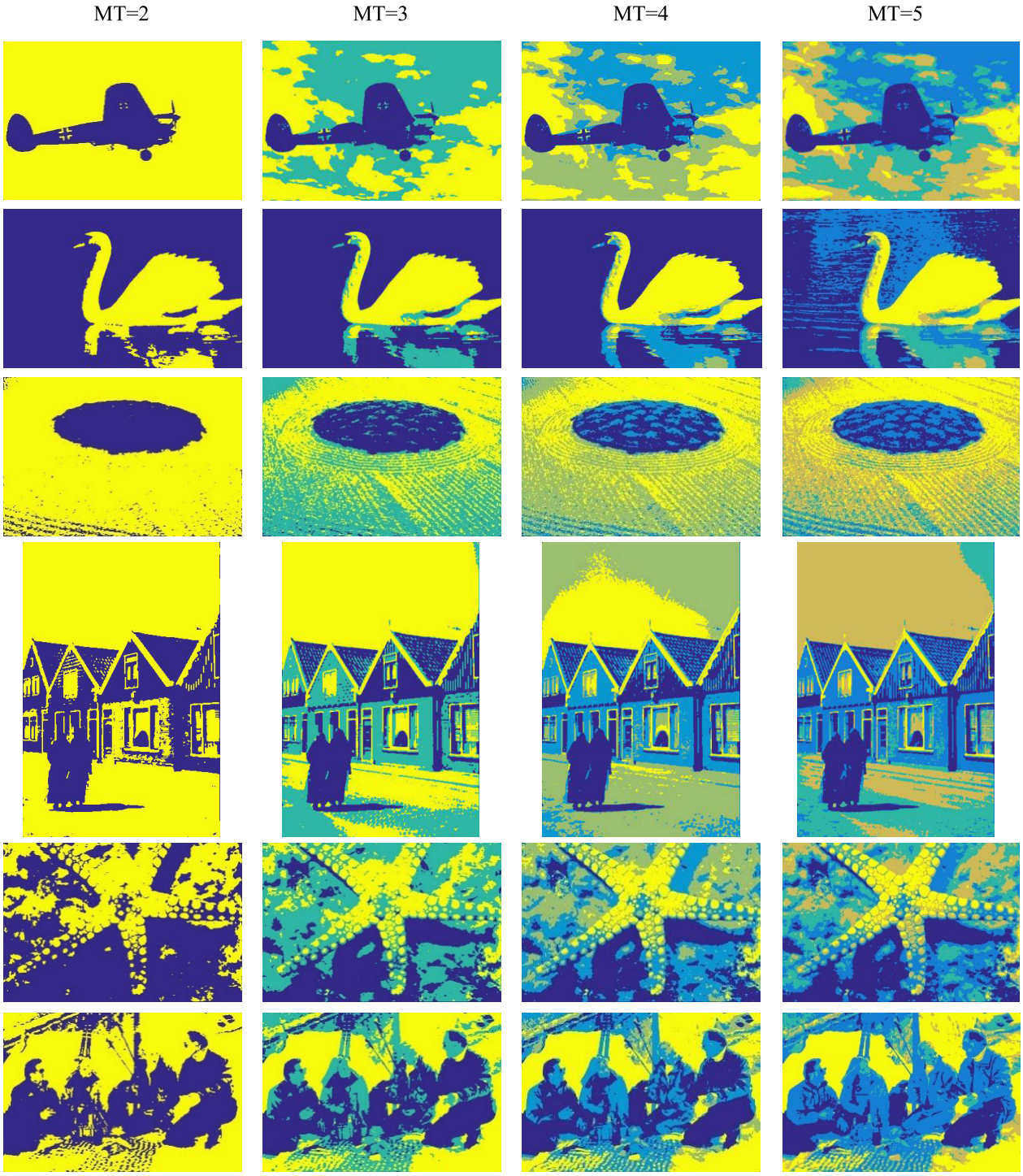

FIGURE 3. The segmentation results based on FCOA.

FSIM values) on the image Filter, Goose and Picnic, whereas on the image Shrub, Community and Starfish, fuzzy Kapur entropy method achieves relatively higher segmentation quality, but the difference between them is small. The difference in terms of PSNR is basically within 0.5, whereas the difference in terms of FSIM is not more than 0.1. However, when the threshold number exceeds 3, the fuzzy Kapur entropy-based method is better than Otsu method in PSNR comparison. Only on Community image with threshold number of 4 and on Picnic image with threshold number of 3, PSNR and FSIM values are slightly higher in the Otsu method, which is 0.0239 and 0.3395 respectively. In FSIM value comparison, with the increase of threshold number, fuzzy Kapur entropy method also performs better.

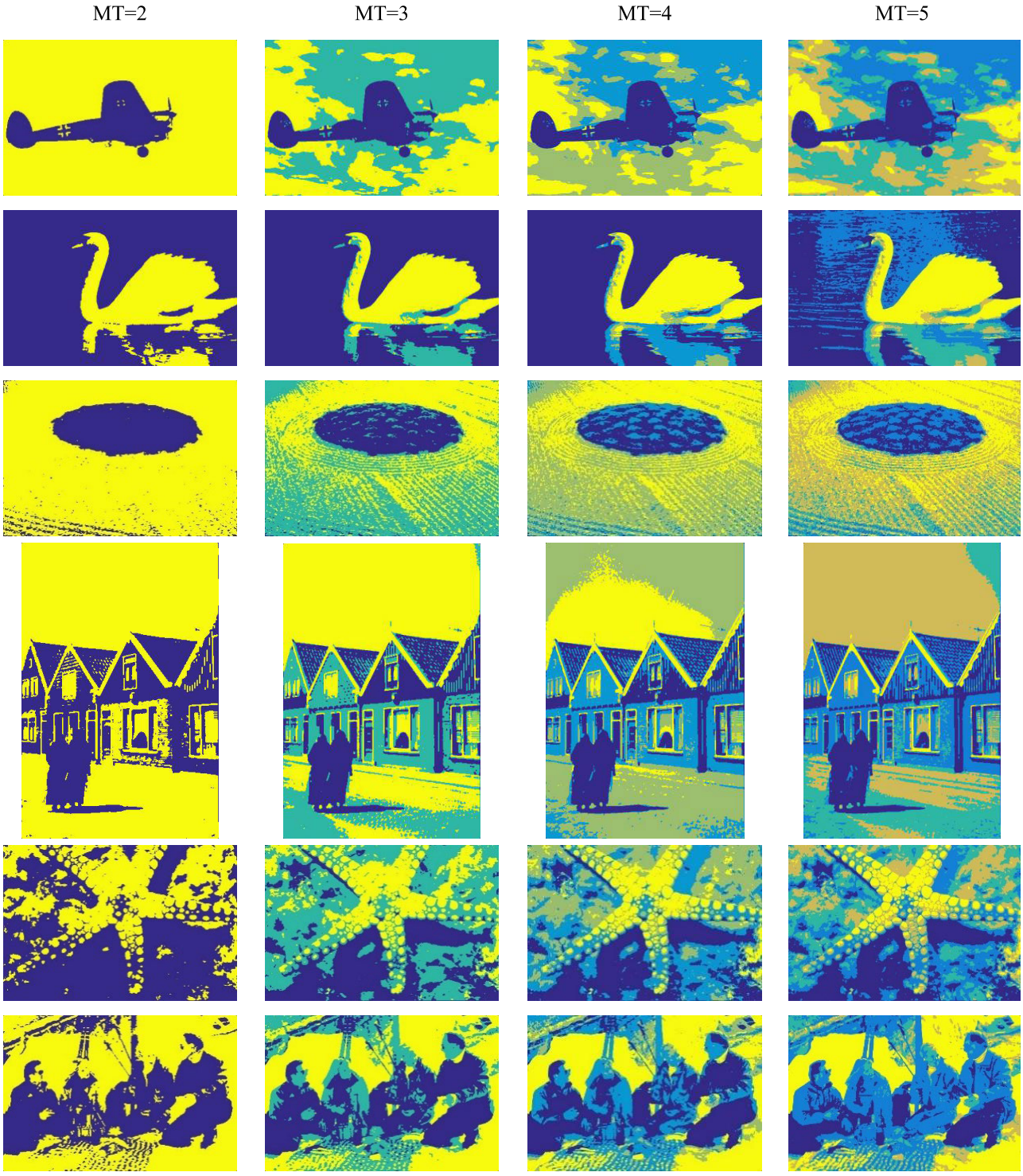

FIGURE 4. The segmentation results based on FICOA.

D. COMPARISON OF IMAGE THRESHOLDING RESULT BETWEEN FICOA AND FCOA

By comparison of different objective functions, fuzzy Kapur entropy method obtains better image segmentation quality. Next, we will take fuzzy Kapur entropy as the objective function to compare the effect of FCOA and FICOA in MT image segmentation. In order to present the image segmentation results more precisely, this article constructs the index image according to the region of the gray image after thresholding segmentation, and then transform the index image into RGB color image. Figure 3 and Figure 4 show the segmentation results of FCOA and FICOA with different threshold

TABLE 5. The results of FICOA with fuzzy kapur objective function.

Image	MT	Thresholds	PSNR	FSIM
Fighter	2	36.5 164	17.0304	0.6974
	3	37.5 113.5 203.5	**20.2354**	**0.7231**
	4	42.5 118 162.5 215	**21.3911**	0.7227
	5	38.5 104.5 152 185 223.5	**21.8223**	**0.7422**
Goose	2	63 159	18.3296	**0.5927**
	3	72.5 132.5 199.5	**22.6667**	**0.6178**
	4	62.5 110.5 163 218.5	**24.7063**	**0.6393**
	5	32 65 118 180 223	**25.9682**	**0.7660**
Shrub	2	68 178	**18.7046**	0.2705
	3	70.5 141 198.5	**19.8846**	0.5768
	4	62 112 139.5 199	**20.3340**	0.6381
	5	55 110 136 162 194	**20.6468**	**0.6916**
Community	2	58 170.5	**18.2341**	**0.5565**
	3	55 114 186	**20.0420**	**0.6311**
	4	51 107.5 156 205	20.7285	0.6591
	5	41 100 131 170 226	**21.2949**	**0.7128**
Starfish	2	62.5 184.5	17.4745	**0.5096**
	3	50.5 106 182.5	**19.9855**	0.5838
	4	43 92.5 136 194	**21.5972**	**0.6617**
	5	39 87 115.5 161.5 212	**22.8617**	**0.7177**
Picnic	2	82 164	16.3730	0.5568
	3	77.5 141.5 199.5	20.5767	0.6573
	4	68 138 172.5 218	**22.8883**	**0.7199**
	5	71 122.5 157.5 190 228	**24.2068**	**0.7647**

TABLE 6. The results of FCOA with fuzzy kapur objective function.

Image	MT	Thresholds	PSNR	FSIM
Fighter	2	36.5 164	17.0304	0.6974
	3	37.5 117.5 207.5	20.2317	0.7244
	4	36.5 116.5 159.5 211	21.2451	0.7286
	5	37.5 102 143.5 180.5 219.5	21.5796	0.7326
Goose	2	62 158.5	18.2777	0.5929
	3	73.5 125 190	22.5160	0.6172
	4	65 113 163.5 217.5	24.5372	0.6392
	5	36.5 68.5 108.5 163.5 216	25.7511	0.7596
Shrub	2	68 178	18.7046	0.2705
	3	72 144 200	19.8229	0.5747
	4	60.5 116.5 139.5 201.5	**20.3457**	0.6372
	5	47.5 103.5 128.5 156 208	20.4858	0.6796
Community	2	58 170.5	18.2341	0.5565
	3	61.5 123 189	19.8398	0.6188
	4	56 116 159 212.5	20.6621	0.6550
	5	47 106.5 139 173.5 227	21.2194	0.7050
Starfish	2	62.5 184.5	17.4745	0.5096
	3	59 118 187	19.9262	0.5908
	4	41.5 114 147 202.5	21.5150	0.6542
	5	40.5 91.5 127.5 164.5 215.5	22.6405	0.7114
Picnic	2	81.5 163	16.2816	0.5562
	3	69 139 197	20.4172	0.6512
	4	56.5 133 167.5 218.5	22.8660	0.7174
	5	67.5 122.5 153 185.5 224.5	24.0739	0.7645

numbers. From the comparison, it can be observed that bi-level thresholding can effectively separate the main object from the background, and with the increase of threshold

TABLE 7. Comparison of image thresholding result by PSNR with different methods.

Image	MT	PSNR				
		GWO	FMQABCA	FMDGWOA	FCOA	FICOA
Fighter	2	12.7187	16.9651	17.0304	17.0304	17.0304
	3	16.0551	20.1362	20.1923	20.2317	**20.2354**
	4	17.0224	21.2674	21.3002	21.2451	**21.3911**
	5	18.8665	21.5475	21.5529	21.5796	**21.8223**
Goose	2	15.0182	17.5107	18.2777	18.2777	**18.3296**
	3	16.6803	20.3213	**22.6895**	22.5160	22.6667
	4	18.3412	23.5738	24.5940	24.5372	**24.7063**
	5	19.0864	24.6911	25.9070	25.7511	**25.9682**
Shrub	2	15.1397	18.6683	18.7046	18.7046	18.7046
	3	16.4273	18.1700	19.8764	19.8229	**19.8846**
	4	17.3642	20.1456	20.2809	20.3457	**20.3340**
	5	18.9998	20.4251	20.4727	20.4858	**20.6468**
Community	2	16.0747	18.2300	18.2341	18.2341	18.2341
	3	18.2495	19.7287	19.8886	19.8398	**20.0420**
	4	18.4678	20.7181	20.6289	20.6621	**20.7285**
	5	20.2214	21.2815	**21.3067**	21.2194	21.2949
Starfish	2	14.9845	17.4140	17.4140	17.4745	**17.4745**
	3	17.3068	19.7241	19.8708	19.9262	**19.9855**
	4	19.2231	19.7407	21.5804	21.5150	**21.5972**
	5	20.8924	22.6369	22.6734	22.6405	**22.8617**
Picnic	2	13.6951	16.2002	16.2816	16.2816	**16.3730**
	3	16.9100	20.4477	20.5450	20.4172	**20.5767**
	4	19.7884	22.6588	22.6998	22.8660	**22.8883**
	5	20.4981	24.1301	23.9350	24.0739	**24.2068**

number, the image segmentation accuracy improves gradually. From the perspective of the optimization effect of FCOA and FICOA, they obtain relatively similar segmentation results in visual effect, so it is difficult to judge the merits of the two methods subjectively. Therefore, the evaluation parameters based on FCOA are given in Table 6.

In comparison with Table 5 and Table 6 FICOA achieves slightly higher PSNR and FSIM values than or similar to FCOA when the threshold number is 2. However, when the threshold number increases, the PSNR value of FICOA is higher than that of FCOA except for the Shrub image when the threshold number is 4. Overall, the FICOA has increased by an average of 0.45% compared with the FCOA, and particularly increased by 0.2427, an increase of 1.12% on the Fighter image when the threshold number is 5. In terms of FSIM comparison, FICOA has an average increase of 0.4% over FCOA. Although FCOA is slightly higher than FICOA in some cases, it is only 0.0118 higher at the most. Therefore, the comprehensive performance of FICOA in image segmentation quality is better by comparison of detailed evaluation indices.

E. COMPARISON OF IMAGE THRESHOLDING RESULT BY PSNR

With the increasing application of SIOA in multilevel thresholding segmentation, it is difficult to tell the advantages and

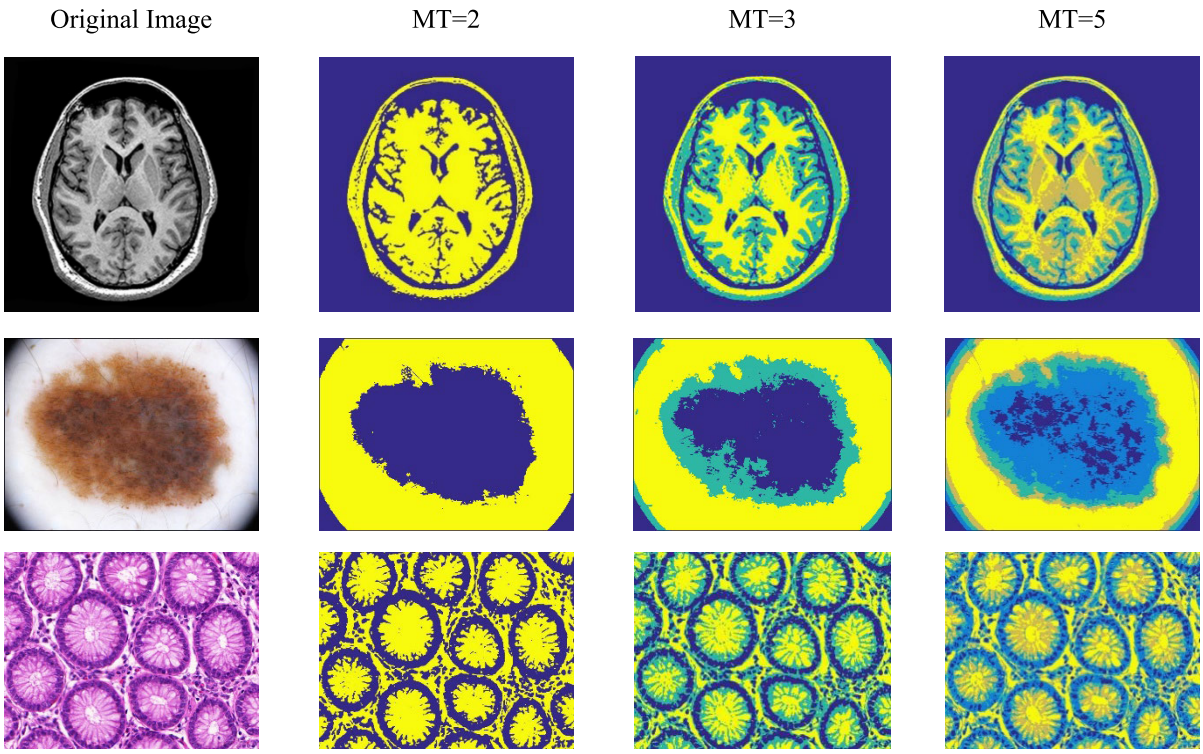

FIGURE 5. The medical segmentation results based on FICOA.

disadvantages of these algorithms only from visual effects. The comparison between Figure 3 and Figure 4 fully illustrates this point. Therefore, in this article we use PSNR and FSIM to compare the algorithm effect quantitatively. However, the comparative references [13], [14], [25] mentioned in this article all use PSNR as the main evaluation criterion, so we will compare the performance of GWO, FMQABCA, FMDGWOA, FCOA and FICOA in terms of PSNR. The relevant data are shown in Table 7. Notably, due to the difference between the computer and the Matlab version, before the relevant data of GWO, FMQABCA, FMDGWOA are obtained, we try to use the data in the original reference. Only when the results obtained using the software and hardware in this paper's setting are better than the original, we choose to use the data calculated on our platform.

This article not only applies FCOA to MT segmentation for the first time, but also improves it to FICOA. Therefore, in the performance analysis, we compare FCOA and FICOA with other three algorithms quantitatively. Compared with GWO, FCOA achieves higher PSNR values in all images under any threshold condition. The PSNR value of FCOA achieves an average increase of 3.2353, improves by 19.06% on average, by 34.99% at the highest, by 4.94% at the lowest. Compared with FMQABCA, the PSNR value of FCOA achieves an average increase of 0.3894, an average increase by1.94%, the highest increase of 10.8%. However, the PSNR values of Fighter, Community and Picnic images are slightly lower than FMQABCA. Compared with FMDGWOA, FCOA has obtained similar evaluation results, and there is no distinction between them.

In Section V.C, we have compared and analyzed the performance of FCOA and FICOA, so in this section we only compare FICOA with GWO, FMQABCA and FMDGWOA. Compared with GWO, FICOA also obtained higher PSNR values in all pictures and under any threshold condition. And the PSNR value of FICOA achieves an average increase of 3.3313, improves by 19.58% on average, by 36.06% at the highest, 5.31% at the lowest. Compared with FMQABCA, the PSNR value of FICOA achieves an average increase of 0.4854, an average increase by 2.39%, the highest increase of 11.54%, and the lowest increase of 0.023%. Compared with FMDGWOA, the PSNR value of FICOA achieves an average increase of 0.0853, the highest increase of 0.2718, an average increase by 0.4%, the highest increase by 01.25%. All data compared, we find that the PSNR of FMDGWOA only on the Goose and Community are slightly higher when the threshold number is 3 and 5 respectively.

Compared with [13], [14], [25], FCOA and FICOA in this article are significantly better than GWO, FMQABCA, and slightly better than FMDGWOA in segmentation effects. Particularly, the advantages of FCOA and FICOA are more obvious when compared with the same kind of swarm intelligence optimization algorithms like GWO, which further proves that the fuzzy median aggregation method shows significant effects.

According to the data analysis of Tables 4 to 7, the fuzzy Kapur entropy-based FICOA has achieved the best image segmentation effect, With the visual comparison of Figure 3 and Figure 4, FICOA is further proved to be an efficient MT segmentation method.

TABLE 8. The results of FICOA with different thresholds.

Image	MT	Thresholds	PSNR	FSIM
Brain	2	53 154	18.2564	0.6299
	3	39 98 188.5	22.5939	0.7821
	5	13 52 102.5 151.5 213	25.7788	0.8913
Lesion	2	74 201.5	16.4347	0.6676
	3	77.5 155 205	17.9287	0.7125
	5	55 103 158 187.5 224.5	18.4735	0.7459
Colon	2	80 207.5	13.3887	0.5657
	3	73.5 147 201.5	13.8709	0.7361
	5	47 108 139.5 172.5 222.5	14.1456	0.8493

F. EXPERIMENTAL EFFECT OF FICOA METHOD IN MEDICAL IMAGE PROCESSING

Medical image segmentation can effectively help doctors to make computer-aided diagnosis, set out surgical planning, dynamically simulate the structure of human tissues or organs, and analyze the structure of lesions. so multilevel thresholding segmentation is widely used in medical image processing. In order to verify the effect of FICOA in medical image segmentation, three kinds of medical images are tested in our work.

Figure 5 shows the original images of Brain, Lexion tissue and Colon medical images and their segmentation results when the threshold number is set to 2,3,5 respectively. It can be seen from the figure that when the threshold number is 2, FICOA can clearly reflect the tissue structure of medical image, and as the threshold number increases, the tissue structure of medical image will become clearer and finer.

Table 8 lists the threshold values, PSNR and FSIM values generated in the segmentation process of three medical images. As can be seen from these data, the PSNR and FSIM values of these images increase significantly as the threshold number increases, which confirms the segmentation effect in Figure 5.

V. CONCLUSION

In this article, the COA is applied to multilevel thresholding segmentation for the first time, which is further improved through a differential scaling factor. The image segmentation results with Otsu and fuzzy Kapur entropy as the objective functions are compared and analyzed. From the analysis of the experimental data, the FICOA based on fuzzy Kapur entropy obtains better image segmentation quality. In particular, the fuzzy median aggregation is applied to refine the segmentation results so that isolated points or over-segmentation can be avoided in the process. Compared with GWO, FMQABCA and FMDGWOA, FCOA and FICOA methods have certain advantages in visual effects and PSNR, FSIM evaluation indices, especially when compared to the same kind of wolf evolution algorithm GWO, FCOA And FICOA methods show significant advantages. In the end, we also discussed the application of the FICOA method in medical image segmentation. From the visual effects and quantitative data of Brain, Lesion tissue and Colon medical images, FICOA can effectively extract the tissue or texture structure of medical images, and can be effectively applied to assist medical diagnosis. In the future, we will continue to try the application of the COA in medical image segmentation and recognition, and strive to propose a completer and more effective medical image segmentation framework.

REFERENCES

[1] M. Sezgin and B. Sankur, "Survey over image thresholding techniques and quantitative performance evaluation," *J. Electron. Imag.*, vol. 13, no. 1, pp. 146–168, 2004.
[2] M. Omari and S. O. Jaafri, "Application of image compression to multiple-shot pictures using similarity norms with three level blurring," *Comput. Mater. Continua*, vol. 59, no. 3, pp. 753–776, 2019.
[3] F. D. Martino and S. Sessa, "PSO image thresholding on images compressed via fuzzy transforms," *Inf. Sci.*, vol. 506, pp. 308–324, Jan. 2020.
[4] Z. Pan, X. Yi, Y. Zhang, B. Jeon, and S. Kwong, "Efficient in-loop filtering based on enhanced deep convolutional neural networks for HEVC," *IEEE Trans. Image Process.*, vol. 29, pp. 5352–5366, 2020.
[5] Z. Yan, W. Xu, and C. Yang, "A power thresholding function-based wavelet image denoising method," *J. Imag. Sci. Technol.*, vol. 62, no. 1, pp. 1–11, 2018.
[6] K. Jin and S. Wang, "Image denoising based on the asymmetric Gaussian mixture model," *J. Internet Things*, vol. 2, no. 1, pp. 1–11, 2020.
[7] S. Susan and K. M. Rachna Devi, "Text area segmentation from document images by novel adaptive thresholding and template matching using texture cues," *Pattern Anal. Appl.*, vol. 23, no. 2, pp. 869–881, May 2020.
[8] S. Bandyopadhyay, S. Das, and A. Datta, "A hybrid fuzzy filtering–fuzzy thresholding technique for region of interest detection in noisy images," *Int. J. Speech Technol.*, vol. 50, no. 4, pp. 1112–1132, Apr. 2020.
[9] Z. Pan, X. Yi, Y. Zhang, H. Yuan, F. L. Wang, and S. Kwong, "Frame-level bit allocation optimization based on video content characteristics for HEVC," *ACM Trans. Multimedia Comput., Commun., Appl.*, vol. 16, no. 1, pp. 1–20, Apr. 2020.
[10] M. A. E. Aziz, A. A. Ewees, and A. E. Hassanien, "Whale optimization algorithm and moth-flame optimization for multilevel thresholding image segmentation," *Expert Syst. Appl.*, vol. 83, pp. 242–256, Oct. 2017.
[11] S. Pare, A. Kumar, G. K. Singh, and V. Bajaj, "Image segmentation using multilevel thresholding: A research review," *Iranian J. Sci. Technol., Trans. Elect. Eng.*, vol. 44, no. 1, pp. 1–29, 2020.
[12] M. A. Elaziz, S. Bhattacharyya, and S. Lu, "Swarm selection method for multilevel thresholding image segmentation," *Expert Syst. Appl.*, vol. 138, Dec. 2019, Art. no. 112818.
[13] L. Li, L. Sun, J. Guo, C. Han, and S. Li, "Fuzzy multilevel image thresholding based on modified quick artificial bee colony algorithm and local information aggregation," *Math. Problems Eng.*, vol. 2016, pp. 1–18, 2016.
[14] L. Li, L. Sun, W. Kang, J. Guo, C. Han, and S. Li, "Fuzzy multilevel image thresholding based on modified discrete grey wolf optimizer and local information aggregation," *IEEE Access*, vol. 2016, pp. 6438–6450, Jan. 2016.
[15] B. Küçüküğurlu and E. Gedikli, "Symbiotic organisms search algorithm for multilevel thresholding of images," *Expert Syst. Appl.*, vol. 147, Jun. 2020, Art. no. 113210.
[16] M. A. Elaziz, A. A. Ewees, and D. Oliva, "Hyper-heuristic method for multilevel thresholding image segmentation," *Expert Syst. Appl.*, vol. 146, May 2020, Art. no. 113201.
[17] Z. Xing, "An improved emperor penguin optimization based multilevel thresholding for color image segmentation," *Knowl.-Based Syst.*, vol. 194, Apr. 2020, Art. no. 105570.
[18] L. He and S. Huang, "An efficient krill herd algorithm for color image multilevel thresholding segmentation problem," *Appl. Soft Comput.*, vol. 89, Apr. 2020, Art. no. 106063.
[19] B. Wu, J. Zhou, X. Ji, Y. Yin, and X. Shen, "An ameliorated teaching–learning-based optimization algorithm based study of image segmentation for multilevel thresholding using Kapur's entropy and Otsu's between class variance," *Inf. Sci.*, vol. 533, pp. 72–107, Sep. 2020.
[20] M. S. R. Naidu, P. Rajesh Kumar, and K. Chiranjeevi, "Shannon and fuzzy entropy based evolutionary image thresholding for image segmentation," *Alexandria Eng. J.*, vol. 57, no. 3, pp. 1643–1655, Sep. 2018.

[21] Z. Yang and A. Wu, "A non-revisiting quantum-behaved particle swarm optimization based multilevel thresholding for image segmentation," *Neural Comput. Appl.*, vol. 32, no. 16, pp. 12011–12031, Aug. 2020.
[22] A. K. Bhandari, A. Kumar, S. Chaudhary, and G. K. Singh, "A novel color image multilevel thresholding based segmentation using nature inspired optimization algorithms," *Expert Syst. Appl.*, vol. 63, pp. 112–133, Nov. 2016.
[23] O. Tarkhaneh and H. Shen, "An adaptive differential evolution algorithm to optimal multi-level thresholding for MRI brain image segmentation," *Expert Syst. Appl.*, vol. 138, Dec. 2019, Art. no. 112820.
[24] S. Zhang, W. Jiang, and S. Satoh, "Multilevel thresholding color image segmentation using a modified artificial bee colony algorithm," *IEICE Trans. Inf. Syst.*, vol. 101, no. 8, pp. 2064–2071, 2018.
[25] A. K. M. Khairuzzaman and S. Chaudhury, "Multilevel thresholding using grey wolf optimizer for image segmentation," *Expert Syst. Appl.*, vol. 86, pp. 64–76, Nov. 2017.
[26] Y. Xue, T. Tang, W. Pang, and A. X. Liu, "Self-adaptive parameter and strategy based particle swarm optimization for large-scale feature selection problems with multiple classifiers," *Appl. Soft Comput.*, vol. 88, Mar. 2020, Art. no. 106031.
[27] J. Pierezan and L. Dos Santos Coelho, "Coyote optimization algorithm: A new Metaheuristic for global optimization problems," in *Proc. IEEE Congr. Evol. Comput. (CEC)*, Jul. 2018, pp. 1–8.
[28] R. C. T. de Souza, C. A. de Macedo, L. dos Santos Coelho, J. Pierezan, and V. C. Mariani, "Binary coyote optimization algorithm for feature selection," *Pattern Recognit.*, vol. 107, Nov. 2020, Art. no. 107470.
[29] H. M. Sultan, A. S. Menesy, S. Kamel, and F. Jurado, "Developing the coyote optimization algorithm for extracting parameters of proton-exchange membrane fuel cell models," *Elect. Eng.*, vol. 2020, pp. 1–15, Sep. 2020, doi: 10.1007/s00202-020-01103-6.
[30] J. Arfaoui, H. Rezk, M. Al-Dhaifallah, M. N. Ibrahim, and M. Abdelkader, "Simulation-based coyote optimization algorithm to determine gains of PI controller for enhancing the performance of solar PV water-pumping system," *Energies*, vol. 13, no. 17, p. 4473, 2020.
[31] L. Shen, X. Chen, Z. Pan, K. Fan, F. Li, and J. Lei, "No-reference stereoscopic image quality assessment based on global and local content characteristics," *Neurocomputing*, vol. 424, pp. 132–142, Feb. 2021, doi: 10.1016/j.neucom.2020.10.024.

LINGUO LI was born in Tai'an, Shandong, China, in 1982. He received the B.S. degree in computer science and technology from Liaocheng University, in 2005, the M.S. degree in computer application technology from Jiangnan University, in 2008, and the Ph.D. degree in information network from the Nanjing University of Posts and Telecommunications, China. From 2008 to 2017, he was a Lecturer with Fuyang Normal University, where he has been an Assistant Professor with the School of Information Engineering, since 2017. His research interests include image processing and swarm intelligence optimization algorithm.

LIJUAN SUN received the B.S. degree in radio engineering from Southeast University, in 1985, and the M.S. degree in signal, circuit and system and the Ph.D. degree in communication and information system from the Nanjing University of Posts and Telecommunications, Nanjing, China, in 1988 and 2007, respectively.

She is currently a Professor and a Ph.D. Supervisor with the School of Computer Science and Technology and the School of Software, Nanjing University of Posts and Telecommunications. Her research interests include multimedia wireless sensor networks and evolutionary computation.

YU XUE (Member, IEEE) received the Ph.D. degree from the School of Computer Science and Technology, Nanjing University of Aeronautics and Astronautics, China, in 2013. He was a Visiting Scholar with the Victoria University of Wellington, Wellington, New Zealand, from 2016 to 2017. He is currently an Associate Professor with the School of Computer and Software, Nanjing University of Information Science and Technology. He is also a Visiting Scholar with the Department of Computer Science and Engineering, Michigan State University, East Lansing, USA. He has published more than 20 journal and conference papers. His research interests include evolutionary computation, feature selection, adaptive search, and evolutionary machine learning. He is a member of ACM and CCF.

SHUJING LI received the B.S. degree in computer science and technology from Liaocheng University, in 2005, and the M.S. degree in computer application technology from the China University of Geosciences, in 2008. From 2008 to 2017, she was a Lecturer with Fuyang Normal University, where she has been an Assistant Professor with the School of Information Engineering, since 2017. Her research interests include evolutionary computation and image and video processing.

XUWEN HUANG received the B.S. degree in network engineering from the Zhengzhou Institute of Aeronautical Industry Management, in 2018. He is currently pursuing the master's degree with the School of Computer and Information Engineering, Fuyang Normal University, Fuyang, China. His research interests include evolutionary computation and image and video processing.

ROMANY FOUAD MANSOUR received the B.S. and M.S. degrees in computer science and the Ph.D. degree from Assiut University, Egypt, in 1998, 2006, and 2009, respectively. He is currently working as an Associate Professor with the Department of Mathematics, Faculty of Science, New Valley University, Egypt. His research interests include pattern recognition, computer vision, computer networks, soft computing, image processing, evolutionary computation, and machine learning.